

2-Pyridinethiol/2-Pyridinethione Tautomeric Equilibrium. A Comparative Experimental and Computational Study

Damian Moran,^{†,‡} Kengkaj Sukcharoenphon,[§] Ralph Puchta,[‡] Henry F. Schaefer, III,[†]
Paul v. R. Schleyer,^{*,†,‡} and Carl D. Hoff^{*,§}

Center for Computational Quantum Chemistry, University of Georgia, Athens, Georgia 30602,
Computer Chemistry Center, Universität Erlangen-Nürnberg, Henkestrasse 42,
D-91054 Erlangen, Germany, and the Department of Chemistry, University of Miami,
Coral Gables, Florida 33124

schleyer@chem.uga.edu; choff@jaguar.ir.miami.edu

Received August 30, 2002

The gas phase and solvent dependent preference of the tautomerization between 2-pyridinethiol (**2SH**) and 2-pyridinethione (**2S**) has been assessed using variable temperature Fourier transform infrared (FTIR) experiments, as well as ab initio and density functional theory computations. No spectroscopic evidence (ν_{S-H} stretch) for **2SH** was observed in toluene, C_6D_6 , heptane, or methylene chloride solutions. Although, C_s **2SH** is 2.61 kcal/mol more stable than C_s **2S** (CCSD(T)/cc-pVTZ//B3LYP/6-311+G(3df,2p)+ZPE), cyclohexane solvent-field relative energies (IPCM-MP2/6-311+G(3df,2p)) favor **2S** by 1.96 kcal/mol. This is in accord with the FTIR observations and in quantitative agreement with the -2.6 kcal/mol solution (toluene or C_6D_6) calorimetric enthalpy for the **2S/2SH** tautomerization favoring the thione. As the intramolecular transition state for the **2S**, **2SH** tautomerization (**2TS***) lies 25 (CBS-Q) to 30 kcal/mol (CCSD/cc-pVTZ) higher in energy than either tautomer, tautomerization probably occurs in the hydrogen bonded dimer. The B3LYP/6-311+G(3df,2p) optimized C_2 **2SH** dimer is 10.23 kcal/mol + ZPE higher in energy than the C_{2h} **2S** dimer and is only 2.95 kcal/mol + ZPE lower in energy than the C_2 **2TS*** dimer transition state. Dimerization equilibrium measurements (FTIR, C_6D_6) over the temperature range 22–63 °C agree: $K_{eq}^{298} = 165 \pm 40 M^{-1}$, $\Delta H = -7.0 \pm 0.7$ kcal/mol, and $\Delta S = -13.4 \pm 3.0$ cal/(mol deg). The difference between experimental and B3LYP/6-311+G(3df,2p) [-34.62 cal/(mol deg)] entropy changes is due to solvent effects. The B3LYP/6-311+G(3df,2p) nucleus independent chemical shifts (NICS) are -8.8 and -3.5 ppm 1 Å above the **2SH** and **2S** ring centers, respectively, and the thiol is aromatic. Although the thione is not aromatic, it is stabilized by the thioamide resonance. In solvent, the large **2S** dipole, 2–3 times greater than **2SH**, favors the thione tautomer and, in conclusion, **2S** is thermodynamically more stable than **2SH** in solution.

Introduction

The tautomerization between 2-hydroxypyridine and 2-pyridone is a classic medium-dependent equilibrium: whereas the hydroxy form is favored in the gas phase and the enol tautomer favored in high dielectric solvents, comparable amounts of both are present in nonpolar solvents such as cyclohexane.¹ Although less studied than their oxygen analogues, there is evidence that the thione/thiol tautomeric equilibrium (Figure 1) between 2-pyridinethiol (**2SH**) and 2-pyridinethione (**2S**) also strongly depends on the environment: **2S** is generally believed to be more stable in polar solvents^{2–6} and **2SH** in

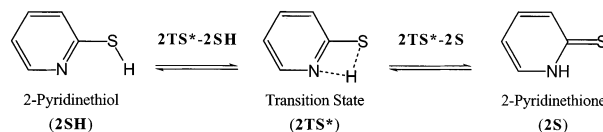


FIGURE 1. Thiol/thione tautomeric equilibrium.

nonpolar solvents and the gas phase.^{7,8} On the basis of matrix isolation infrared spectroscopic studies, which assumed that **2SH** condensed from the gas phase and had a 2610 cm^{-1} ν_{S-H} band, Nowak et al.⁹ concluded that **2SH** was ~ 2.4 kcal/mol more stable than **2S**. X-ray crystallography shows that a **2S** hydrogen bonded dimer (**[2S]₂**) is the solid state form.^{10,11} A **2S** dimer, similar to

[†] University of Georgia.

[‡] Universität Erlangen-Nürnberg.

[§] University of Miami.

(1) Wong, M. W.; Wiberg, K. B.; Frisch, M. J. *J. Am. Chem. Soc.* **1992**, *114*, 1645.

(2) Beak, P. *Acc. Chem. Res.* **1977**, *10*, 186.

(3) Beak, P.; Covington, J. B. *J. Am. Chem. Soc.* **1978**, *100*, 3961.

(4) Beak, P.; Covington, J. B.; Smith, S. G.; White, J. M.; Zeigler, J. *M. J. Org. Chem.* **1980**, *45*, 1354.

(5) Katritzky, A. R.; Jug, K.; Oniciu, D. C. *Chem. Rev.* **2001**, *101*, 1421.

(6) Schank, A.; Dereppe, J. M.; Meerssche, M. V. *Bull. Soc. Chim. Belg.* **1983**, *92*, 199.

(7) Stoyanov, S.; Stoyanova, T.; Akrivos, P. D.; Karagiannidis, P.; Nikolov, P. *J. Heterocycl. Chem.* **1996**, *33*, 927.

(8) Beak, P.; Covington, J. B.; White, J. M. *J. Org. Chem.* **1980**, *45*, 1347.

(9) Nowak, M. J.; Lapinski, L.; Rostkowska, H.; Les, A.; Adamowicz, L. *J. Phys. Chem.* **1990**, *94*, 7406.

TABLE 1. Literature Reported 2S/2SH Computed Tautomeric Preferences (kcal/mol)^a

	PG	2SH favored	2S favored	ref
HF/6-31G(d) ^b	C ₁		0.85	13
HF/6-31++G(d,p) ^b	C ₁		0.41	13
MP2/6-31G(d) ^b	C ₁		0.65	13
B3LYP/6-31G(d,p) + ZPE	C _s		0.77	12
MP2/6-31G(d,p) + ZPE	C _s	2.99		12
MP4/6-31G(d,p) + ZPE ^c	C _s	2.19		12
HF/3-21G(d) + ZPE ^d	C _s		4.87	9
HF/DZP + ZPE ^d	C _s	4.20		9
MBPT/DZP + ZPE ^d	C _s	6.81		9

^a Unless otherwise specified, geometries, energies and ZPE corrections are computed at the same level. ^b HF/6-31G(d) geometry. ^c HF/6-31G(d,p) geometry and ZPE. ^d HF/3-21G(d) geometry and ZPE.

the solid-state structure, also forms in concentrated solutions with nonpolar solvents.¹⁰

Computations on **2S** and **2SH** show that the relative energies depend strongly on the basis set, zero point vibrational energy (ZPE) and electron correlation (Table 1). Nowak et al.⁹ found **2S** to be 4.87 kcal/mol more stable at HF/3-21G(d) + ZPE but **2SH** was preferred by 4.20 (HF/DZP + HF/3-21G(d) ZPE) and 6.81 kcal/mol (MPBT2/DZP + HF/3-21G(d) ZPE) at higher levels. Kwiatkowski et al.¹² reported **2S** to be 0.77 kcal/mol more stable than **2SH** at B3LYP/6-31G(d,p) + ZPE but 2.99 kcal/mol less stable at MP2/6-31G(d,p) + ZPE and 2.19 kcal/mol less stable at MP4(SDQ)/6-31G(d,p)//HF/6-31G(d,p) + ZPE. More recently, Armstrong et al.¹³ reported **2S** to be 0.41 (HF/6-31++G(d,p)) and 0.65 kcal/mol (MP2/6-31G(d)) more stable, but their results seem questionable.¹⁴

From both theoretical and experimental points of view, the **2S/2SH** tautomerization reaction presents challenges. Computational studies of sulfur-containing molecules often show large basis set effects.^{15–19} For example, in their study of sulfine, CH₂=S=O, Ruttink et al.²⁰ found G1 and G2 relative energies unacceptable because of the inadequate 6-31G(d) basis set used for geometry optimizations. Turecek¹⁵ reported that C₂H₆OS and C₂H₇OS⁺ relative energies were unreliable at B3LYP/6-31+G(d,p) and B3LYP/6-311G(d,p) but that geometries did not change significantly when re-optimized at B3LYP/6-311+G(2df,2p). The **2S/2SH** tautomerization also presents experimental challenges. Due to the relatively low S–H bond molar absorptivity, there are conflicting

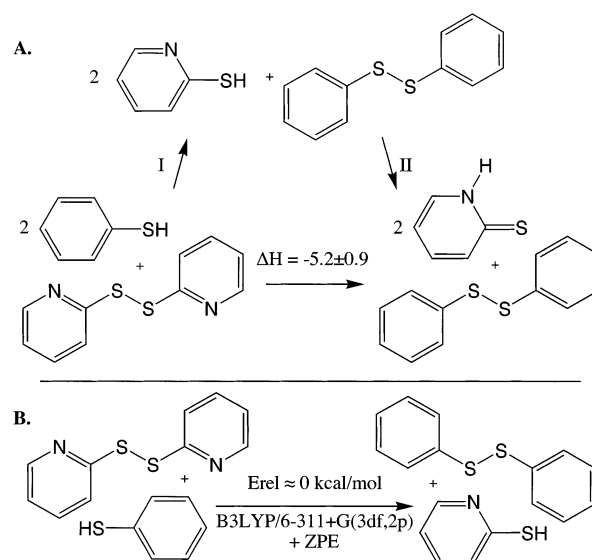


FIGURE 2. Equation for the reaction between thiophenol and 2,2'-pyridine disulfide. Part A, step I is assumed to have zero heat loss, as shown by the isodesmic equation in part B. The overall reaction enthalpy, therefore, corresponds to the **2SH** → **2S** tautomerization enthalpy (kcal/mol).

reports²¹ regarding the existence of a **2SH** ν_{S–H} stretching frequency at low concentrations and in nonpolar environments. In addition, **2S** presents experimental difficulties because it is sensitive to photochemical and oxidative decomposition, with 2,2'-dipyridine disulfide forming at varying rates.^{7,9} Because agreement between earlier computational and experimental reports on the **2SH** and **2S** tautomeric preference is lacking, we now revisit the problem.

Results and Discussion

Tautomerization Enthalpy: Thiophenol + 2,2'-Dipyridine Disulfide Reaction. An approximate **2S/2SH** tautomerization enthalpy can be derived from calorimetric data for the reaction between thiophenol and 2,2'-dipyridine disulfide in toluene solution, 2C₆H₅SH + C₅H₄N–SS–C₅H₄N → C₆H₅–SS–C₆H₅ + 2**2S** (Figure 2). The reaction enthalpy (ΔH_{obs}; average of five measurements) is –10.0 ± 0.4 kcal/mol and under these conditions, using K_{eq} = 137 M⁻¹ for the monomer/dimer equilibrium at 30 °C (see below), the solution contains ~32% monomer and ~68% dimer. The enthalpy corresponding to 100% **2S** monomer is calculated by adding 4.8 ± 0.5 kcal/mol [68% of the 7.0 ± 0.7 kcal/mol endothermic dissociation energy (see below)] to ΔH_{obs} and ΔH = –5.2 ± 0.9 kcal/mol for the reaction shown in the bottom line of the thermochemical cycle in Figure 2A. This value is the sum of two hypothetical steps (see Figure 2): (I) **2SH** formation and (II) **2SH** tautomerizing to **2S**. However, step I is approximately thermoneutral (see the isodesmic reaction in Figure 2B) and step II, tautomerization of two moles **2SH** to **2S**, is responsible for the reaction enthalpy. Hence, on the basis of the cycle in Figure 2, we estimate that in solution (toluene, C₆D₆) the tautomerization favors **2S** by approximately 2.6 kcal/

(10) Ohms, U. H.; Guth, A.; Kutoglu, A.; Scheringer, C. *Acta Crystallogr. B* **1982**, *38*, 831.

(11) Penfold, B. R. *Acta Crystallogr.* **1953**, *6*, 707.

(12) Kwiatkowski, J. S.; Leszczynski, J. L. *J. Mol. Struct.* **1996**, *376*, 325.

(13) Armstrong, D. R.; Davies, J. E. D.; Feeder, N.; Lamb, E.; Longridge, J. L.; Rawson, J. M.; Snaith, R.; Wheatley, A. E. H. *J. Mol. Model.* **2000**, *6*, 234.

(14) Armstrong et al. (2000) did not compare their results to Nowak et al. (1990) or Kwiatkowski et al. (1996). Frequencies for their C₁ optimized structures (including transition states) were not detailed. Relative energies were not ZPE corrected, which can contribute ~2.5 kcal/mol (Kwiatkowski et al. (1996)).

(15) Turecek, F. *J. Phys. Chem. A* **1998**, *102*, 4703.

(16) Xantheas, S.; Dunning, T. H., Jr. *J. Phys. Chem.* **1993**, *97*, 6616.

(17) Smart, B. A.; Schiesser, C. H. *J. Comput. Chem.* **1995**, *16*, 1055.

(18) Frank, A. J.; Sadilek, M.; Ferrier, J. G.; Turecek, F. *J. Am. Chem. Soc.* **1996**, *118*, 11321.

(19) Frank, A. J.; Sadilek, M.; Ferrier, J. G.; Turecek, F. *J. Am. Chem. Soc.* **1997**, *119*, 12343.

(20) Ruttink, P. J. A.; Burgers, P. C.; Francis, J. T.; Terlouw, J. K. *J. Phys. Chem.* **1996**, *100*, 9694.

(21) Lautie, A.; Hervieu, J.; Belloc, J. *Spectrochim. Acta A* **1983**, *39*, 367.

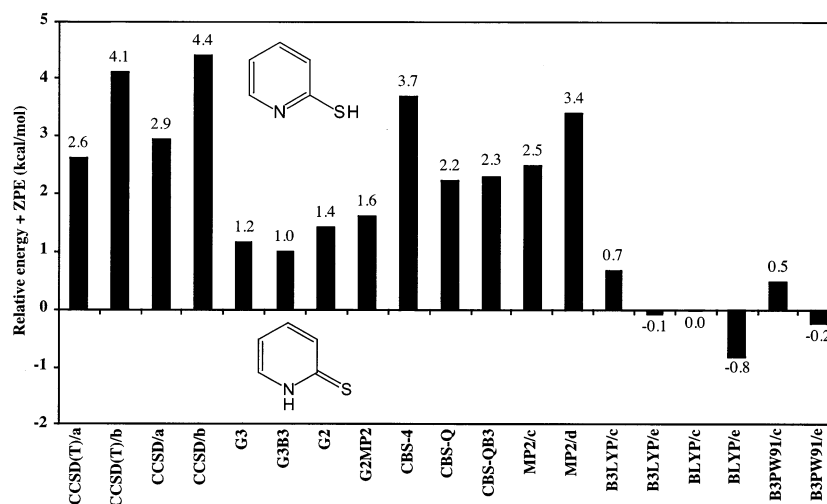


FIGURE 3. ZPE corrected gas phase relative energy difference ($2S-2SH$, kcal/mol) between $2SH$ and $2S$. Basis set key: a = cc-pVTZ; b = cc-pVDZ; c = 6-311+G(3df,2p); d = 6-311+G(2d,p); e = 6-311+G(d,p). ZPE and absolute energies included in Tables S1 and S2. Coupled cluster energies are corrected using a ZPE of 2.56 kcal/mol, which is the average of (B3LYP, BLYP, B3PW91)/6-311+G(3df,2p) zero point energies.

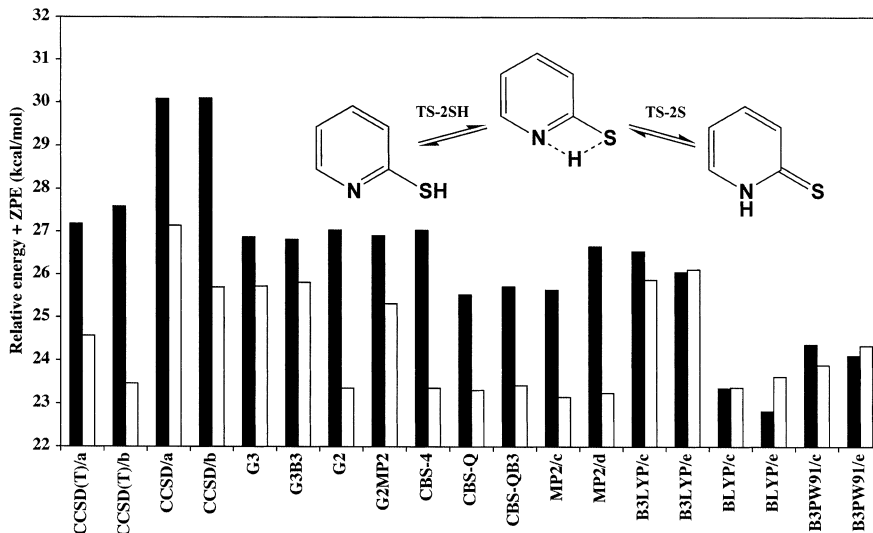


FIGURE 4. ZPE corrected barrier to monomeric thiol/thione tautomer interconversion. Solid bars (left) are for the forward $2TS^*-2SH$ and hashed bars (right) for reverse $2TS^*-2S$ reactions. Basis set key: a = cc-pVTZ; b = cc-pVDZ; c = 6-311+G(3df,2p); d = 6-311+G(2d,p); e = 6-311+G(d,p). Energies and ZPE included in Tables S1 and S2. Coupled cluster energies are corrected using a ZPE of 2.56 kcal/mol, which is the average of (B3LYP, BLYP, B3PW91)/6-311+G(3df,2p) zero point energies.

mol. This estimate corresponds to $K_{eq} \approx 100$, favoring the thione, and is consistent with both the theoretical solution phase enthalpic preference (see below) and our failure to spectroscopically observe $2SH$ in solution (see below).

Computed Tautomeric Stability. Large variations in the computed tautomerization energy, ranging from -6.81 to $+4.87$ kcal/mol, have been reported (Table 1). Here, we attempt to establish a more definitive relative energy estimate for $2SH$, $2S$, and the transition state connecting the two ($2TS^*$), by employing more sophisticated basis sets and electron correlation methods. ZPE corrected relative energy differences between tautomers ($2S-2SH$; kcal/mol) are plotted in Figure 3; barriers to intramolecular proton transfer ($2TS^*-2SH$ and $2TS^*-2S$; kcal/mol) are plotted in Figure 4. Absolute energies, ZPE, and relative energies are summarized in Tables

S1–S3, Supporting Information. Figure 3 shows that ZPE strongly favors the thiol tautomer (cf. non-ZPE corrected relative energies plotted in Figure S4, Supporting Information), reflecting the N–H bond strength relative to S–H. Coupled cluster energies were zero point corrected using the average DFT/6-311+G(3df,2p) ZPE (2.56 kcal/mol). Though $2SH$ has one imaginary frequency ($71.1i$ cm^{-1}) at MP2/6-311+G(d,p), this disappeared at MP2/6-311+G(2d,p). The barriers to intramolecular proton transfer (Figure 4), which range from 22 to 30 kcal/mol are large but do not preclude gas phase unimolecular tautomerization.

CCSD(T)/cc-pVTZ + ZPE favors $2SH$ by 2.61 kcal/mol and the gas phase tautomer stability difference is almost entirely due to ZPE. Gaussian-2, Gaussian-3, and CBS calculations, which are less expensive than coupled cluster, agree. G3 theory, accurate to approximately 1

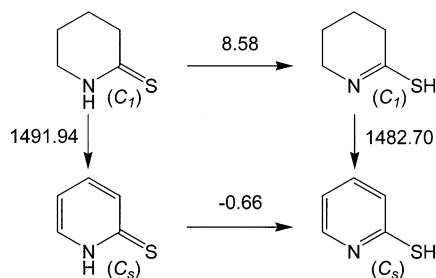


FIGURE 5. Competing influence of thioamide resonance and aromaticity on **2S** and **2SH** tautomeric stability. B3LYP/6-311+G(3df,2p)//B3LYP/6-311+G(3df,2p) + ZPE relative energies (kcal/mol) shown.

kcal/mol²² finds the thiol most stable by 1.15 kcal/mol. **2SH** also is preferred at MP2/6-311+G(2d,p) + ZPE by 3.4 kcal/mol. Reviewing Table 1, it appears that previous computations incorporating electron correlation and ZPE were correct, even though geometries and ZPE were Hartree–Fock computed. Kwiatkowski et al.'s¹² HF/3-21G(d) **2SH** ↔ **2S** Δ ZPE was 2.60 kcal/mol, which was in excellent agreement with Lapinski et al.'s²³ 2.82 kcal/mol experimental ZPE and our 2.56 kcal/mol DFT/6-311+G(3df,2p) ZPE. The **2SH**, **2S** relative energies are very small, ranging from ~0 to 3.7 kcal/mol. Wong et al.¹ reported that 2-hydroxypyridine is favored by between 2.77 (MP2/6-31+G(d,p)) and 0.01 kcal/mol (MP4SDQ/6-31+G(d,p)), and our small energy gaps are reasonable. A more recent QCISD/6-311+G(2d,p) estimate places the enol 1.12 kcal/mol lower in energy than the keto tautomer.²⁴ Figure 5 shows the origin of the small **2SH**, **2S** tautomeric energy gap, which results from the competition between thione thioamide resonance^{25,26} and thiol aromatic stabilization (see NICS below). The thioamide resonance stabilizes the thione by 6.46 kcal/mol relative to the thiol, whereas cyclic electron delocalization stabilizes **2SH** by 7.12 kcal/mol relative to **2S**.

ZPE uncorrected DFT energies favor **2S** (Figure S4). Inclusion of ZPE to the DFT/6-311+G(d,p) relative energy does not switch their favored tautomer. The ZPE corrected BLYP/6-311+G(3f,2p) relative energy is zero, whereas B3LYP and B3PW91, both incorporating Becke's B3 exchange functional,²⁷ favor **2SH** by 0.5–0.7 kcal/mol. These small energy differences are beyond the accuracy of DFT and we cannot recommend DFT for computing the relative energies of such tautomeric systems. In contrast, DNA base tautomerization energies,^{28–30} which are on the order ≥ 8 kcal/mol, are well suited to DFT and significantly faster for these large systems.³¹ HC(X)YH

(22) Schleyer, P. v. R.; Allinger, N. L.; Clark, T.; Gasteiger, J.; Kollman, P. A.; Schaefer, H. F., III; Schreiner, P. R. *The Encyclopedia of Computational Chemistry*; John Wiley & Sons, Ltd.: Chichester, U.K., 1998.

(23) Lapinski, L.; Nowak, M. J.; Fulara, J.; Les, A.; Adamowicz, L. *J. Phys. Chem.* **1992**, *96*, 6250.

(24) Wolken, J. K.; Turecek, F. *J. Phys. Chem. A* **1999**, *103*, 6268.

(25) Wiberg, K. B.; Rablen, P. R. *J. Am. Chem. Soc.* **1995**, *117*, 2201.

(26) Wiberg, K. B.; Rush, D. J. *J. Am. Chem. Soc.* **2001**, *123*, 2038.

(27) Becke, A. D. *J. Chem. Phys.* **1993**, *98*, 5648.

(28) Leszczynski, J. In *The Encyclopedia of Computational Chemistry*; Schleyer, P. v. R., Allinger, N. L., Clark, T., Gasteiger, J., Kollman, P. A., Schaefer, H. F., III, Schreiner, P. R., Eds.; John Wiley & Sons: Chichester, U.K., 1998; pp 2951–2960.

(29) Yekeler, H.; Ozbakir, D. *J. Mol. Model.* **2001**, *7*, 103.

(30) Rueda, M.; Luque, F. J.; Lopez, J. M.; Orozco, M. *J. Phys. Chem. A* **2001**, *105*, 6575.

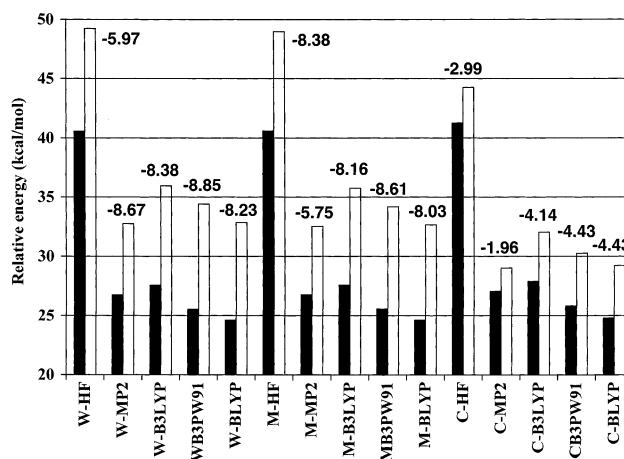


FIGURE 6. Water, methanol, and cyclohexane IPCM-XX/6-311+G(3df,2p)//XX/6-311+G(3df,2p) (XX = HF, MP2, B3LYP, B3PW91, BLYP) **2TS***–**2SH** (solid bars, left), **2TS***–**2S** (hashed bars, right), and **2S**–**2SH** (labeled) relative energies (kcal/mol). Energies included in Table S3.

(X, Y = O, S) formic acid derivative B3LYP/6-311+G(2d,2p) and MP2/6-311+G(2d,2p) tautomeric relative energies are comparable;³² however, the agreement between our MP2 and DFT energies is less satisfactory and clouded by the relative errors intrinsic in both methods.

IPCM-XX/6-311+G(3df,2p)//XX/6-311+G(3df,2p) (XX = HF, MP2, B3LYP, B3PW91, BLYP) solvent field single points, summarized in Figure 6, are at first somewhat surprising. **2S**, which has an MP2/6-311+G(3df,2p) dipole (6.3 D) thrice **2SH** (2.2 D), is the preferred tautomer in water and methanol by 8.7 and 8.4 kcal/mol, respectively. In cyclohexane, a nonpolar solvent with a dielectric of only 2.02, **2S** also is preferred. The IPCM-MP2/6-311+G(3df,2p) cyclohexane relative stability (–1.96 kcal/mol) is in gratifyingly good agreement with our experimental ΔH (3.5 kcal/mol). In view of the large computed intramolecular hydrogen transfer barriers, dimerization provides an alternative path to **2S/2SH** tautomerization.

Tautomer Searching: 2S FTIR. Characteristic spectral features of the variable temperature **2S** FTIR spectral data are shown in Figure 7 and summarized in Table 2. The 2400–2600 cm^{-1} region was searched over a wide concentration range, but in none of the solvent systems was it possible to identify an assignable S–H band above background noise. In addition, NMR spectroscopy did not detect an S–H proton signal. Attempts to determine the gas phase FTIR spectrum of **2S** were unsuccessful due to the low vapor pressure of the hydrogen bridged dimeric solid. The dominance of **2S** is in contrast with the behavior of hydroxy tautomers, 2-hydroxypyridine, and 2-pyridone, where comparable amounts of both are present in nonpolar solvents such as cyclohexane.¹ **2S** bleaching was observed to occur in the presence of light and oxygen, as has been reported

(31) There is evidence that some gas phase cytosine and guanine compounds exist as mixtures of tautomers and their small tautomerization energies favor the more populated enol forms (Brown, R. D.; Godfrey, P. D.; McNaughton, D.; Pierlot, A. P. *J. Phys. Chem.* **1989**, *93*, 2308. Lapinski, L.; Nowak, M. J.; Fulara, J.; Les, A.; Adamowicz, L. *J. Phys. Chem.* **1990**, *94*, 6555).

(32) Jemmis, E. D.; Giju, K. T.; Leszczynski, J. *J. Phys. Chem. A* **1997**, *101*, 7389.

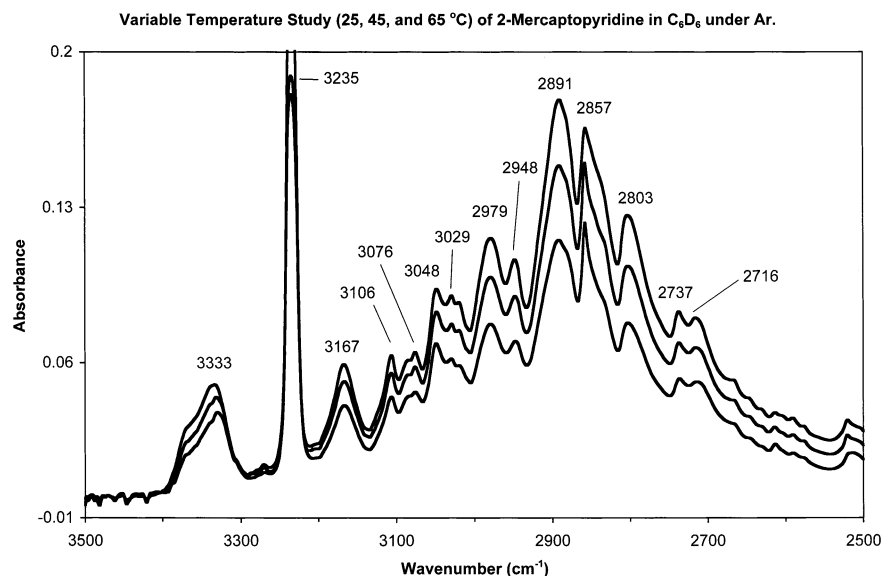


FIGURE 7. **2S** variable temperature FTIR in C_6D_6 at 25 °C (lowest trace), 45 °C, and 65 °C (top trace), showing the region 3500–2500 cm^{-1} . The broad band at 3333 cm^{-1} assigned to the N–H stretch of monomeric **2S** increases with increasing temperature. The manifold of peaks centered at 2891 cm^{-1} and assigned to the **[2S]₂** dimer decreases with increasing temperature

TABLE 2. Characteristic **2S** IR Frequencies (ν ; cm^{-1})

	C_6D_6	CH_2Cl_2	heptane
2S ν_{N-H}	3333	3355 ^a	3384
[2S]₂ ^b	2891, ...	2897, ... ^c	^d

^a Deuteration shifted to 2493 cm^{-1} . ^b Complex series of bands due to hydrogen bonded **[2S]₂** dimer. ^c Deuteration shifted to 2222 cm^{-1} . ^d Due to solvent interference, the **[2S]₂** series were unresolvable in heptane.

elsewhere,⁹ and we conclude that other spectroscopic reports claiming **2SH** observation are most likely spurious and due to decomposition/oxidation in solution. Interestingly, it has been recently reported³³ that FTIR data on benzthiazoline-2-thione indicate that bands earlier assigned to an S–H stretch were in fact C=S stretch overtones. Although not studied as extensively as **2S**, FTIR studies of 2-quinoline thione (**2QS**) (Figure S5) and 8-quinoline thiol (**8QSH**) (Figure S6) provide additional insight regarding the **2S** FTIR shown in Figure 7. The spectrum of **2QS** shows a strong resemblance to that of **2S**, and it is clear that a monomer–dimer equilibrium exists for this thione as well. In low temperature nitrogen and argon matrixes, **2QS** is preferred 7:1 over its thiol tautomer³⁴ and in solution the balance still (not surprisingly) strongly favors the thione. In contrast, the **8QSH** spectrum has an intense 2527 cm^{-1} S–H band, no N–H stretch, and it is clear from Figure S6 that there is little if any thione tautomer present. On the basis of these spectroscopic observations, we conclude that in solution *no significant amounts of 2S or 2QS thiol tautomer are present and that only the 8QSH thiol form is present.*

2S Dimerization. The variable temperature spectra in Figure 7 allow calculation of K_{eq} for the **2S** monomer/dimer equilibrium. Increasing temperature causes an

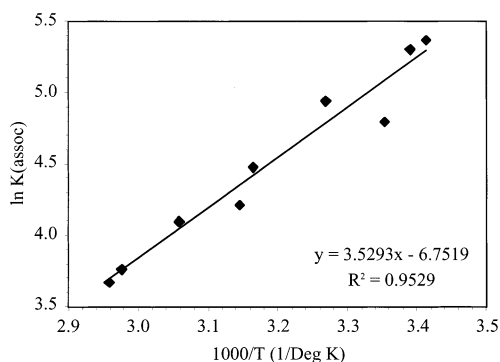


FIGURE 8. **2S** dimerization temperature dependence. log of association constant versus inverse temperature is plotted. Values included in Table S7.

increase in the monomeric **2S** band at 3333 cm^{-1} , with a concomitant decrease in the manifold of peaks centered at 2891 cm^{-1} assigned to the hydrogen bonded dimer. Equilibrium constants were calculated on the basis of absorbance changes using both peak height and area methods and are available in Table S7. A plot of $\ln K_{eq}$ versus $1/T$ (Figure 8) gives a reasonably straight line over the temperature range 18–63 °C and in C_6D_6 solvent at 298 K: $K_{eq}^{298} = 165 \pm 40 M^{-1}$, $\Delta H = -7.0 \pm 0.7$ kcal/mol, and $\Delta S = -13.4 \pm 3.0$ cal/(mol K). The **2S** dimerization equilibrium constant compares reasonably well with data for other thiones studied by Griffiths.³⁵ For example, K_{eq}^{298} for benzthiazoline-2-thione dimerization is $570 \pm 60 M^{-1}$ in CCl_4 . Direct comparison to our data is not possible, because the thermodynamics of the hydrogen bonded adduct formation are solvent dependent.³⁶

Thermodynamic parameters for the monomer/dimer equilibrium (Figure 9) are similar to other data reported

(33) Böhlig, H.; Ackermann, M.; Billes, F.; Kudra, M. *Spectrochim. Acta A* **1999**, *55*, 2635.

(34) Prusinowska, D.; Lapinski, L.; Nowak, M. J.; Adamowicz, L. *Spectrochim. Acta A* **1995**, *51*, 1809.

(35) Griffiths, P. J. F.; Morgan, G. D.; Ellis, B. *Spectrochim. Acta A* **1972**, *38*, 1899.

(36) Spencer, J. N.; Andrefsky, J. C.; Grushow, A.; Naghdi, J.; Patti, L. M.; Trader, J. F. *J. Phys. Chem.* **1987**, *91*, 1673.

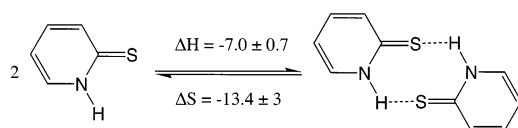


FIGURE 9. Experimentally determined **2S** dimerization thermodynamic parameters (kcal/mol). The B3LYP/6-311+G(3df,2p) entropy change is -34.62 cal/mol deg.

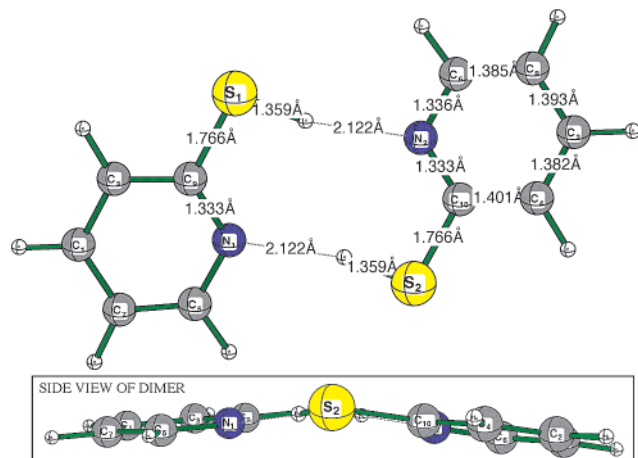


FIGURE 10. B3LYP/6-311+G(3df,2p) optimized **[2SH]₂** (C_2). The $N-C_\alpha-N'-C_{\alpha'}$ dihedral is $\sim 11^\circ$.

for hydrogen bonding. For example, $\Delta H = -7.1$ kcal/mol and $\Delta S = -15.2$ cal/(mol K) for parafluorophenol and pyridine hydrogen bonded adduct formation in CCl_4 .³⁷ Note that the *p*-fluorophenol/pyridine adduct includes only one hydrogen bond, whereas the -7.0 kcal/mol **2S** dimerization enthalpy change corresponds to the formation of two $C=S\cdots H-N$ hydrogen bonds i.e., $\Delta H = -3.5$ kcal/mol per hydrogen bond. However, this lower hydrogen bonding enthalpy is consistent with the reduced hydrogen bonding ability of sulfur (as either thiol donor or, as in this case, thione acceptor) compared with oxygen.^{38,39}

B3LYP/6-311+G(3df,2p) optimized hydrogen bonded **2S** dimer (**[2S]₂**) and **2SH** dimer (**[2SH]₂**) are shown in Figure 10 and Figure 11, respectively. As expected, **[2S]₂** was a C_{2h} minima, however, planar **[2SH]₂** had one imaginary frequency ($8.8i$ cm^{-1}). Mode following led to a C_2 minima, just 0.03 kcal/mol more stable than the C_{2h} **[2SH]₂** dimer structure. The **[2S]₂** dimer was 15.14 kcal/mol (10.23 kcal/mol + ZPE) more stable than the **[2SH]₂** dimer and 20.87 kcal/mol (13.18 kcal/mol + ZPE) lower in energy than the transition state (**[2TS*]₂**) connecting **[2SH]₂** and **[2S]₂** (Figure 12). The TS is a mere 5.73 kcal/mol (2.95 kcal/mol + ZPE) higher in energy than the **[2SH]₂** dimer and it provides a facile pathway for **2SH** present in a solution to tautomerize to the thermodynamically more stable **2S** via the monomer/dimer equilibrium processes (i.e., dimer promoted tautomerization).

(37) Arnett, E. M.; Joris, L.; Mitchell, E.; Murty, T. S. S. R.; Gorrie, T. M.; Schleyer, P. v. R. *J. Am. Chem. Soc.* **1970**, *92*, 2365.

(38) Del Bene, J. B. In *The Encyclopedia of Computational Chemistry*; Schleyer, P. v. R., Allinger, N. L., Clark, T., Gasteiger, J., Kollman, P. A., Schaefer, H. F., III, Schreiner, P. R., Eds.; John Wiley & Sons: Chichester, U.K., 1998; pp 1263–1286.

(39) March, J. *Advanced Organic Chemistry*, 4th ed.; Wiley-Interscience: New York, 1992.

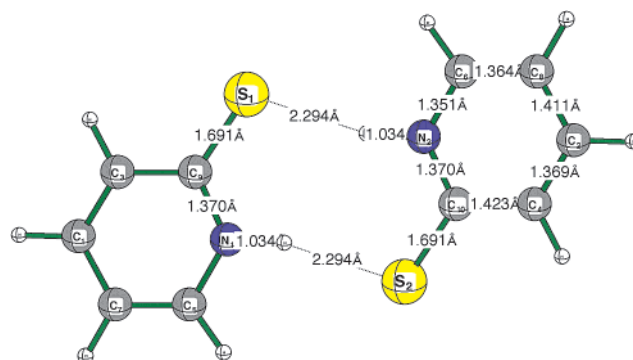


FIGURE 11. B3LYP/6-311+G(3df,2p) optimized **[2S]₂** (C_{2h}). This dimer is 10.23 kcal/mol + ZPE more stable than the **2SH** dimer shown in Figure 10.

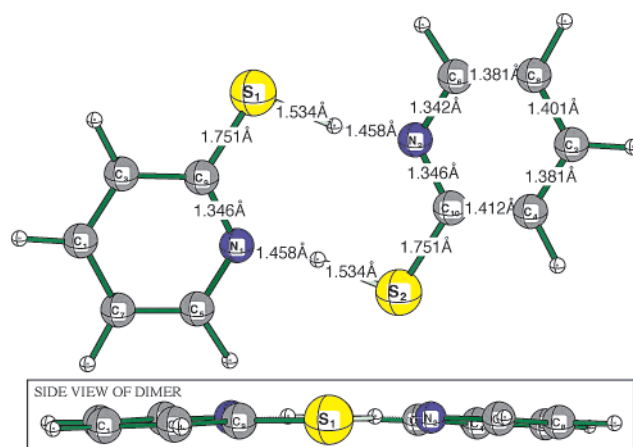


FIGURE 12. B3LYP/6-311+G(3df,2p) optimized **[2TS*]₂** (C_2). The $N-C_\alpha-N'-C_{\alpha'}$ dihedral is $\sim 4^\circ$. This TS is 2.95 kcal/mol + ZPE and 13.18 kcal/mol + ZPE higher in energy than the **[2SH]₂** (Figure 10) and **[2S]₂** (Figure 11) dimers, respectively.

Although largely overlooked subsequently, for example, Umakoshi et al.⁴⁰ and Beak et al.⁴¹ also arrived at this conclusion 20 years earlier. Our experimental solution phase ΔS is -13.0 ± 3.0 cal/(mol deg) and the gas phase B3LYP/6-311+G(3df,2p) entropy change is -34.62 cal/(mol deg). The solvent promotes dimerization, with the 21.62 ± 3.0 cal/(mol deg) reduction in dimerization entropy due to decreased monomer degrees of freedom prior to, and increased solvent disorder upon, dimerization.

Computed Monomer Geometries. As shown in Figure S8 (Supporting Information), the SH proton in **2SH** can exist in either cis or trans conformations. The B3LYP/6-311+G(d,p) optimized bond lengths of both conformers are essentially identical. The $N\cdots H-S$ intramolecular separation is too large for a hydrogen bond;³⁸ however, the slightly smaller $C-S-H$ angle (trans = 96.5° ; cis = 94.3°) suggests a weak electrostatic interaction between the nitrogen and the thiol hydrogen. Indeed, at B3LYP/6-311+G(d,p) + ZPE and MP2/6-311+G(d,p) + ZPE, the cis conformer is preferred by

(40) Umakoshi, K.; Yamasaki, T.; Fukuoka, A.; Kawano, H.; Ichikawa, M.; Onishi, M. *Inorg. Chem.* **2002**, *41*, 4093.

(41) Beak, P.; Bonham, J.; Lee, J. T. *J. Am. Chem. Soc.* **1968**, *90*, 1569.

TABLE 3. Characteristic 2S and 2SH Harmonic Frequencies (ω ; cm^{-1}), IR Intensities (I ; km/mol), and Dipole Moments (debye)

	CCSH to		CSH be		SH st		NH st		dipole (debye)	
	ω_{thiol}	I	ω_{thiol}	I	ω_{thiol}	I	ω_{thione}	I	2SH	2S
MP2 ^a									2.18	6.29
B3LYP ^a	261	19	898	11	2693	3	3571	47	1.99	5.53
B3PW91 ^a	276	20	891	12	2709	4	3588	48	1.95	5.51
BLYP ^a	269	17	866	11	2602	1	3457	34	1.91	5.31
MP2 ^b	203	20	923	13	2773	7	3584	58	2.21	6.31
B3LYP ^c	256	26	897	14	2685	1	3571	50	2.02	5.45
B3PW91 ^c	268	27	891	15	2706	2	3588	51	2.02	5.66
BLYP ^c	261	23	864	14	2592	0.3	3459	34	1.97	5.44

^a 6-311+G(3df,2p). ^b 6-311+G(2d,p). ^c 6-311+G(d,p).

approximately 1.4 kcal/mol. The 2-hydroxypyridine intramolecular N \cdots H–O interaction is worth 5.3 kcal/mol (B3LYP/6-311+G(d,p) + ZPE).

The B3LYP, B3PW91, BLYP, and MP2 optimized geometries of **2SH**, **2S**, and **2TS*** (all using the 6-311+G(3df,2p) basis set) are summarized in Figures S9–S11. These show gas phase heavy atom bond lengths and include optimized N–H and S–H distances. Theoretical studies of sulfur-containing molecules often show large basis set effects;^{15–20} however, the choice of basis set and theoretical method has only a minor affect on optimized **2SH** and **2S** structural parameters (maximum deviation ≤ 0.013 Å). The thione sulfur natural charge is ~ -0.5 e, with a minor contribution (~ 0.1 e) to the **2S** charge distribution from the zwitterionic resonance form.^{25,26} The **2S** optimized bond lengths are in good agreement (≤ 0.058 Å deviation) with the neutron diffraction structure.¹⁰

DFT (B3LYP, B3PW91, and BLYP) and MP2 harmonic frequencies and dipole moments, computed using the 6-311+G(3df,2p) and 6-311+G(2d,p) basis sets, respectively, of characteristic thiol and thione vibrational modes are summarized in Table 3. The **2S** dipole moment is 2.5–3 times greater than **2SH** supporting Nowak et al.'s⁹ conclusion that polar environments favor the thione. In the gas phase, the thione and thiol are stabilized by thioamide bond resonance^{25,26} and cyclic electron delocalization (see below), respectively, and their relative energy difference is negligible.

NICS.^{42–44} The presence of aromaticity in **2SH**, **2S**, and **2TS*** structures was probed by computing B3LYP/6-311+G(3df,2p) shieldings at points in space, so-called NICS, 1 Å above six-membered ring centers (summarized in Figure 13). For reference, the NICS 1 Å above the ring centers of benzene, pyridine, and phenol are -10.1 , -10.1 , and -9.6 ppm, respectively. The **2SH** six-membered ring geometry closely resembles that of *C*_s pyridine C–N (1.334 Å) and C–C (1.390 Å, 1.388 Å) bond lengths, and the **2SH** -8.8 ppm NICS 1 Å above the ring confirms that the thiol is aromatic. In contrast, optimized **2S** has a bond localized structure; with short C3–C4 and C5–C6 bonds, the geometry is consistent with the Lewis structure shown in Figure 1. Furthermore, **2S** NICS 1 Å above the ring is -3.5 ppm, indicating a lack of cyclic

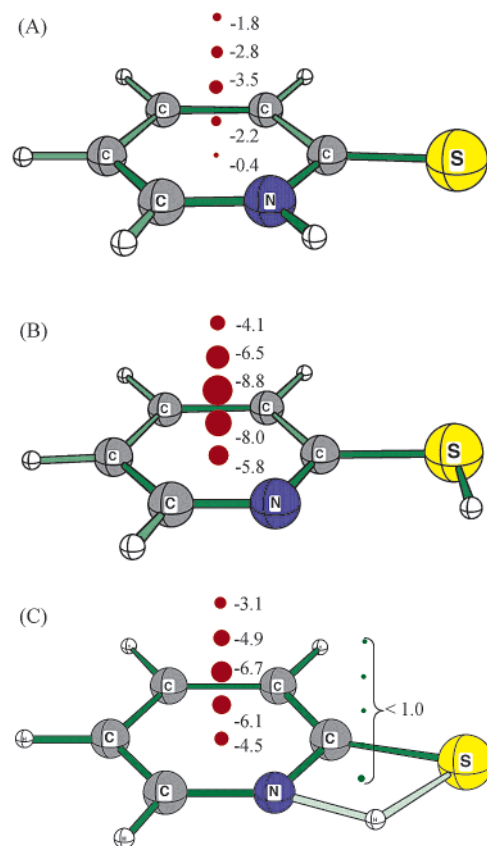


FIGURE 13. **2S** (A), **2SH** (B), and **2TS*** (C) B3LYP/6-311+G(3df,2p) nucleus independent chemical shifts (ppm). Geometries are optimized at the same level. NICS at the center of rings, NICS(0) and at 0.5 Å intervals above rings, NICS(0.5), NICS(1), NICS(1.5), and NICS(2) are shown.

electron delocalization at the ring center. This is in contrast with Cook's⁴⁵ conclusion, based on solvation free energies and equilibrium enthalpies, that **2S** retains most of pyridine's aromatic resonance energy. However, **2TS*** NICS(1) is -6.7 ppm, and the transition state also is aromatic.

Conclusions

In nonpolar solvents there is no FTIR evidence for a significant **2SH** population, and only **2S** is detected. Attempts to measure gas phase FTIR failed due to the low vapor pressure of solid **2S**. The -2.6 kcal/mol solution (toluene or C_6D_6) **2S/2SH** tautomerization enthalpy favors the thione and supports the lack of signature thiol $\nu_{\text{S-H}}$ stretch in FTIR experiments. The -2.4 ± 0.6 kcal/mol calorimetric enthalpy for the **2S/2SH** tautomerization favoring the thione supports the lack of signature thiol $\nu_{\text{S-H}}$ stretch. Computations at a range of levels consistently support a small but significant gas phase **2SH** preference. Relative to *C*_s **2S**, our best level, CCSD(T)/cc-pVTZ/B3LYP/6-311+G(3df,2p)+ZPE, favors *C*_s **2SH** by 2.61 kcal/mol. However, solvent corrected energies shift the balance in favor of **2S**, even in weak hydrocarbon dielectrics such as cyclohexane where the thione is preferred by 1.96 kcal/mol (IPCM-MP2/6-311+G(3df,2p)).

(42) Schleyer, P. v. R.; Maerker, C.; Dransfeld, A.; Jiao, H. J.; Hommes, N. J. r. V. E. *J. Am. Chem. Soc.* **1996**, *118*, 6317.

(43) Schleyer, P. v. R.; Jiao, H.; Hommes, N. J. R. v. E.; Malkin, V. G.; Malkina, O. L. *J. Am. Chem. Soc.* **1997**, *119*, 12669.

(44) Schleyer, P. v. R.; Manoharan, M.; Wang, Z.-X.; Kiran, B.; Jiao, H.; Puchta, R.; Hommes, N. J. R. v. E. *Org. Lett.* **2001**, *3*, 2465.

(45) Cook, M. J.; Tack, R. D.; Linda, P.; Katritzky, A. R. *J. Chem. Soc., Perkin Trans. 2* **1972**, *10*, 1295.

2S oxidation occurred in the presence of light and oxygen, as has been reported and we conclude that other spectroscopic reports claiming **2SH** observation are most likely spurious due to decomposition/oxidation in solution.

As the intramolecular transition state for the **2S**, **2SH** tautomerization (**2TS***) lies 25 (CBS-Q) to 30 kcal/mol (CCSD/cc-pVTZ) higher in energy than either tautomer, tautomerization probably occurs in the hydrogen bonded dimer. The B3LYP/6-311+G(3df,2p) optimized C_2 **2SH** dimer is 10.23 kcal/mol + ZPE higher in energy than C_{2h} **2S** dimer and is only 2.95 kcal/mol + ZPE lower in energy than the C_2 **2TS*** dimer transition state. Dimerization equilibrium measurements over the temperature range 22–63 °C (FTIR, C_6D_6) agree: $K_{eq}^{298} = 165 \pm 40 M^{-1}$, $\Delta H = -7.0 \pm 0.7$ kcal/mol, and $\Delta S = -13.4 \pm 3.0$ cal/(mol deg). The 21.62 ± 3.0 cal/(mol deg) difference between computed and measured entropy changes is due to solvent effects.

NICS are -8.8 and -3.5 ppm 1 Å above the **2SH** and **2S** ring centers, respectively, and the thiol is aromatic. Although the thione is not aromatic, it is stabilized by the thioamide resonance. In solvent, the large **2S** dipole, 2–3 times greater than **2SH**, favors the thione tautomer and, in conclusion, **2S** is thermodynamically more stable than **2SH** in solution. Geometry optimized C_s symmetric **2SH** and **2S** structures are insensitive to basis set and theory level, although ZPE makes a significant difference to the relative stability of the tautomers. For example, the average contribution to the 6-311+G(3df,2p) DFT energies is 2.57 kcal/mol and in the case of B3LYP and B3PW91, enough to switch the relative energy sign in favor of **2SH**.

Knowledge of the tautomeric preference and energetics in this prototype system may provide information as to the intrinsic stability of other thiol/thione tautomers, guiding future experimental efforts.

Materials and Methods

Experimental Details. All manipulations were carried out under argon atmosphere. Solvents were purified using standard techniques. The **[2S]₂** and **[2QS]₂** dimers and so-called “2-pyridinethiol” (“**2SH**”), “2-quinolinethiol” (“**2QS**”), and “8-quinolinethiol” (“**8QSH**”) hydrochloride were recrystallized at -20 °C from CH_2Cl_2 :heptane (1:1). Deuterated **2S** was prepared by stirring a “**2SH**”-saturated methylene chloride solution with excess D_2O overnight. Solutions of “**8QSH**” in C_6D_6 were prepared in situ by adding a small molar excess of pyridine to precipitate pyridinium hydrochloride followed by filtration. 1H NMR spectra were determined in C_6D_6 and C_6D_{12} .

Qualitative FTIR Measurements. “**2S**”, “**2QS**”, and “**8QSH**” (generated in situ from “**8QSH**” hydrochloride by reaction with pyridine) FTIR were collected in C_6D_6 , toluene, CH_2Cl_2 , and heptane.

Attempted Gas Phase FTIR Measurement. A 0.2 g sample of “**2SH**” was added to an evacuated, flame dried 2 L flask. The flask was evacuated and refilled with argon. The procedure was repeated with a second flask except that no “**2SH**” was added. Both flasks were placed on a shaker in the dark for 2 weeks in an attempt to saturate the argon gas with **2S**, **2SH**. The flasks were then connected by butyl rubber tubing through an arcodisk filter to an evacuated 20 m gas cell (at Lawrence-Factor Corp., Miami Lakes) and FTIR collected.

Thiophenol + Pyridine Disulfide Reaction Enthalpy. A liquid mixing cell was loaded in a glovebox with 2 mL of

C_6D_6 solutions of 2-pyridine disulfide (0.024 M, limiting reagent) and thiophenol (0.245 M, $\sim 5\times$ molar excess). The reaction was initiated at 30 °C by rotating the calorimeter. After ~ 3 h, 1H NMR showed **2S** resonances at 13.85 (sb), 7.327 (d) 6.380 (d), 6.216 (t), and 5.483 ppm (t), but residual pyridine disulfide signals (8.17 (d), 7.37 (d), 6.76 (t), 6.33 (t)) were not detected. FTIR showed **2S**/**[2S]₂** bands discussed below. Although the 0.024 M **2S** solution produced by the reaction is near the solubility limit at 30 °C, there was no indication of precipitate in thermograms or immediately after opening the calorimeter cell. Note that although 2 mol of **2S** is produced in the reaction, $2C_6H_5SH + C_5H_4N-SS-C_5H_4N \rightarrow C_6H_5-SS-C_6H_5 + 22S$, the solution is diluted upon mixing and the enthalpy measured corresponds to production of 0.024 M **2S**. Under these conditions and using $K_{eq} = 137 M^{-1}$ (see above), the solution contains 0.0077 M monomer and 0.0081 M dimer.

[2S]₂ Variable Temperature FTIR. Solutions were shielded from light and experiments were performed in low background light conditions. A 5.70 mM solution of **[2S]₂** was prepared in 5.0 mL of C_6D_6 and loaded into a thermostated microreactor, positively pressurized (1.3 atm) with argon. Approximately 90 s was required to collect 100 scans; longer scan times, which can produce local heating of the sample were avoided. To ensure thermal equilibration, measurements were repeated thrice. Returning to low temperature yielded reasonable reproduction of the original spectrum showing minimal decomposition. All measurements were done in transmission mode.

Computational Details. **2SH**, **2S**, and **2TS*** were MP2/6-311+G(2d,p), DFT/6-311+G(d,p), and DFT/6-311+G(3df,2p) (DFT = B3LYP, B3PW91, BLYP) C_s symmetry optimized, and frequencies were computed (at the same level) to characterize stationary points and obtain ZPE's. All frequencies are unscaled. Density functional theory (DFT), in particular B3LYP, have been shown to provide accurate equilibrium geometries and good harmonic vibrational frequencies for a broad range of molecules and ions.^{22,46} MP2/6-311+G(3df,2p) optimizations also were executed. Monomer DFT calculations used a pruned, fine integration grid consisting of 75 radial shells and 302 angular points (75 302). The isodensity polarized continuum model (IPCM)⁴⁷ was used to estimate medium effects on the **2S**/**2SH** tautomer stability. MP2/6-311+G(d,p) and DFT/6-311+G(3df,2p) single points were computed for gas phase optimized geometries (same level) in cyclohexane ($\epsilon = 2.02$), methanol ($\epsilon = 32.63$), and water ($\epsilon = 78.39$) solvent fields. Similarly, B3LYP/6-311+G(3df,2p) nucleus independent chemical shifts (NICS)^{42–44} were computed to probe the ring currents in the optimized (same level) **2SH**, **2S**, and **2TS*** structures. The Gaussian 98 program was used throughout.⁴⁸

2SH, **2S**, and **2TS*** benchmark CCSD(T)//cc-pVDZ and CCSD(T)//cc-pVTZ single points were computed using B3LYP/6-311+G(3df,2p) optimized **2S** and **2SH**,^{49,50} an approach used

(46) Koch, W.; Holthausen, M. C. *A Chemist's Guide to Density Functional Theory*; Wiley-VCH: Weinheim, 2000.

(47) Foresman, J. B.; Keith, T. A.; Wiberg, K. B.; Snoonian, J.; Frisch, M. J. *J. Phys. Chem.* **1996**, *100*, 16098.

(48) Frisch, M. J.; Trucks, G. W.; Schlegel, H. B.; Scuseria, G. E.; Robb, M. A.; Cheeseman, J. R.; Zakrzewski, V. G.; Montgomery, J. A., Jr.; Stratmann, R. E.; Burant, J. C.; Dapprich, S.; Millam, J. M.; Daniels, A. D.; Kudin, K. N.; Strain, M. C.; Farkas, O.; Tomasi, J.; Barone, V.; Cossi, M.; Cammi, R.; Mennucci, B.; Pomelli, C.; Adamo, C.; Clifford, S.; Ochterski, J.; Petersson, G. A.; Ayala, P. Y.; Cui, Q.; Morokuma, K.; Malick, D. K.; Rabuck, A. D.; Raghavachari, K.; Foresman, J. B.; Cioslowski, J.; Ortiz, J. V.; Stefanov, B. B.; Liu, G.; Liashenko, A.; Piskorz, P.; Komaromi, I.; Gomperts, R.; Martin, R. L.; Fox, D. J.; Keith, T.; Al-Laham, M. A.; Peng, C. Y.; Nanayakkara, A.; Gonzalez, C.; Challacombe, M.; Gill, P. M. W.; Johnson, B. G.; Chen, W.; Wong, M. W.; Andres, J. L.; Head-Gordon, M.; Replogle, E. S.; Pople, J. A. *Gaussian 98*, revision A.7; Gaussian, Inc.: Pittsburgh, PA, 1998.

(49) Hehre, W. J.; Radom, L.; Pople, J. A.; Schleyer, P. v. R. *Ab Initio Molecular Orbital Theory*; John Wiley & Sons: New York, 1986.

(50) Foresman, J. B.; Frisch, E. *Exploring Chemistry with Electronic Structure Methods*, 2nd ed.; Gaussian, Inc.: Pittsburgh, PA, 1996.

successfully for the 2-pyridone, 2-pyridol tautomeric equilibrium by Frisch and co-workers.¹ High accuracy⁵¹ Gaussian-3 (G3, G3B3),^{52–54} Gaussian-2 (G2, G2MP2),^{55,56} and complete basis set (CBS-Q, CBS-QB3, CBS-4)⁵⁷ methods, also were included to evaluate the **2S/2SH** tautomeric stability. MP2 and coupled cluster calculations employed the frozen core approximation. Both the theory and methodology of these high level methods have been discussed extensively.^{22,51}

Expecting C_{2h} point groups, **[2SH]₂**, **[2S]₂**, and **[2TS*]₂** dimers were optimized and frequencies computed at B3LYP/6-311+G(d,p) and B3LYP/6-311+G(3df,2p). **[2SH]₂** and **[2TS*]₂** dimers were not C_{2h} minima; mode following led to twisted C_2 dimer structures. The thiol dimer had one small B3LYP/6-

311+G(d,p) imaginary frequency (7.8i cm^{-1}) in D_{2h} symmetry that increased slightly ($\sim 2 \text{ cm}^{-1}$) when the integration grid was increased from p(75 302) to a pruned 99 590 grid p(99 590). Mode following led to a C_2 symmetric thiol dimer, but we were only able to converge the **[2SH]₂** B3LYP/6-311+G(d,p) C_2 optimization using the p(99 590) grid. A B3LYP/6-311+G(3df,2p) NImag=0 dimer structure was computed ($\omega_1 = 7.0 \text{ cm}^{-1}$). **[2S]₂** and **[2TS*]₂** also were computed using the p(99 590) grid for consistency.

Acknowledgment. Support of this work by the University of Georgia and the Petroleum Research Fund administered by the American Chemical Society is gratefully acknowledged. We thank Dr. Frank G. Pühlhofer for several fruitful discussions and a referee for helpful comments and references.

Supporting Information Available: Tables of absolute energies and ZPE are summarized in S1–S3. S4–S11 give FTIR spectra and energy difference graphs, a list of dimerization equilibrium constants, and optimized geometry diagrams. Monomer and dimer geometries, optimized using the 6-311+G(d,p) and 6-311+G(3df,2p) basis sets, are tabulated in S12–S19. This material is available free of charge via the Internet at <http://pubs.acs.org>.

JO0263768

(51) Petersson, G. A.; Malick, D. K.; Wilson, W. G.; Ochterski, J. W.; Montgomery, J. A.; Frisch, M. J. *J. Chem. Phys.* **1998**, *109*, 10570.

(52) Baboul, A. G.; Curtiss, L. A.; Redfern, P. C.; Raghavachari, K. *J. Chem. Phys.* **1999**, *110*, 7650.

(53) Curtiss, L. A.; Redfern, P. C.; Raghavachari, K.; Rassolov, V.; Pople, J. A. *J. Chem. Phys.* **1999**, *110*, 4703.

(54) Curtiss, L. A.; Raghavachari, K.; Redfern, P. C.; Rassolov, V.; Pople, J. A. *J. Chem. Phys.* **1998**, *109*, 7764.

(55) Curtiss, L. A.; Raghavachari, K.; Pople, J. A. *J. Chem. Phys.* **1993**, *98*, 1293.

(56) Curtiss, J. A.; Jones, C.; Trucks, G. W.; Raghavachari, K.; Pople, J. A. *J. Chem. Phys.* **1990**, *93*, 2537.

(57) Montgomery, J. A.; Frisch, A. M. J.; Ochterski, J. W.; Petersson, G. A.; Raghavachari, K.; Zakrzewski, V. G. *J. Chem. Phys.* **1998**, *109*, 6505.